Available online at www.sciencedirect.com
ScienceDirect
Inorganica Chimica Acta 362 (2009) 1011–1021
Inorganica Chimica Acta
www.elsevier.com/locate/ica

Ruthenium-thiobase complexes: Synthesis, spectroscopy, density functional studies for *trans,cis,cis*-[$Ru^{II}(AsPh_3)_2$(*N,S*-2-Thiopyrimidinato)$_2$] and structural analysis of selected weak C–H···N and C–H···S interactions

Gabriella Tamasi [a], Sandra Defazio [a], Luisa Chiasserini [b], Alessandro Sega [b], Renzo Cini [a,*]

[a] *Department of Chemical and Biosystem Sciences and Technologies, University of Siena, Via Aldo Moro 2, I-53100 Siena, Italy*
[b] *Department of Medicinal Chemistry, University of Siena, Via Aldo Moro 2, I-53100 Siena, Italy*

Received 5 April 2007; accepted 21 July 2007
Available online 6 August 2007

This study is dedicated to Professor Dr. Bernhard Lippert, University of Dortmund

Abstract

The reaction of *trans*-[$Ru^{III}(AsPh_3)_2Cl_3(CH_3OH)$] (green powder) with 2-thiopyrimidine-1,3, HTPYM, in ethanol, produced red crystals of *trans,cis,cis*-[$Ru^{II}(AsPh_3)_2$(*N,S*-2-thiopyrimidinato)$_2$]. The compound has two $TPYM^-$ chelating anions in the equatorial plane, whereas the As atoms occupy the apical positions. It is stable in the solid state but the yellow chloroform solutions turn to green quickly in air atmosphere. The Ru–As, Ru–S and Ru–N bond distances average 2.432(1), 2.440(2) and 2.078(6) Å, respectively. The $AsPh_3$ ligands assume a *semi-trefoil* C_1 arrangement and have C–H···S intra-molecular hydrogen bond type interactions to $TPYM^-$ ligands. These latter ligands are also involved in C–H···N and C–H···S interactions that pair two thiobase ligands via an unusual way. Density functional computational studies on [$Ru(AsH_3)_2$(*N,S*-$TPYM)_2$] model molecules show that the *cis,cis,trans* isomer is more stable than the *trans,cis,cis* one by some 5 kcal mol^{-1}.

Keywords: Ruthenium complex; Thiobase; DFT; XRD; Hydrogen bonds

1. Introduction

The synthesis of new "platinum group" complexes with purine/pyrimidine derivatives as ligands or the synthesis of complexes able to react with bio-molecules like aminoacids, nucleobases, proteins, and nucleic acids is a matter that attracts much efforts nowadays because the well-known anti-cancer, anti-metastase, anti-bacterial activity shown by several of analogous species in the past [1–5]. Furthermore, the chemistry of Ru–XR_3 derivatives, where X is a pnictogen element, has much fascinated the community of inorganic chemists in the past half century. Selected fields that were related to these species are basic coordination chemistry, catalysis, electrochemistry, spectroscopy and bio-inorganic chemistry. In spite of the very many scientific reports, much work remains to be done, at least from preparative, spectroscopy, theoretical and reactivity with bio-molecules stand points.

It is known that thiobases like thiopurines and thiopyrimidines have anti-cancer, anti-viral properties by their own [6–9]. Thus, the combination of such ligands with metals like ruthenium and other "block-d" metals could hopefully produce pharmacologically active complexes whose action comes from synergic effects by the metal and the ligand, once the coordination molecule dissociates in the target tissue [2a,10–12].

* Corresponding author.
E-mail address: cini@unisi.it (R. Cini).

0020-1693/$ - see front matter © 2007 Elsevier B.V. All rights reserved.
doi:10.1016/j.ica.2007.07.026

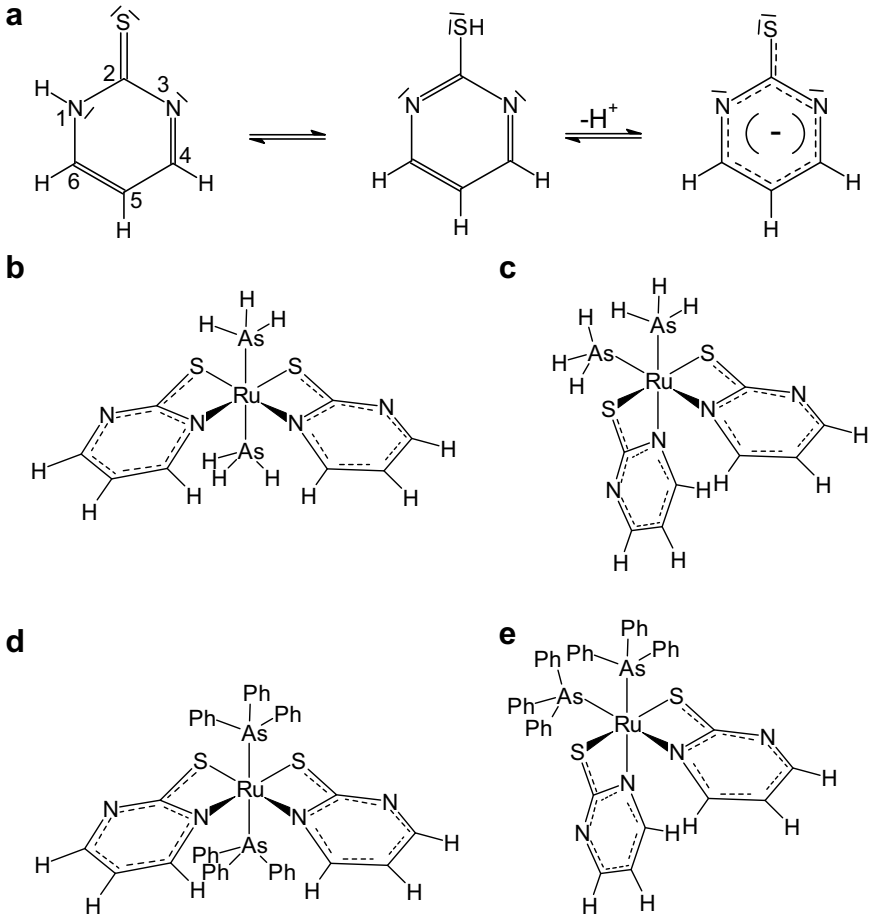

Scheme 1. Sketches for the selected molecules studied in this work. The molecules were also optimized via DFT-B3LYP methods in this work. (a) 2-thiopyrimidine-1,3 (HTPYM). (b) *trans,cis,cis*-[$Ru(AsH_3)_2(\underline{N,S}\text{-TPYM})_2$]. (c) *cis,cis,trans*-[$Ru(AsH_3)_2(\underline{N,S}\text{-TPYM})_2$]. (d) *trans,cis,cis*-[$Ru(AsPh_3)_2(\underline{N,S}\text{-TPYM})_2$] (Ph = phenyl). (e) *cis,cis,trans*-[$Ru(AsPh_3)_2(\underline{N,S}\text{-TPYM})_2$].

Furthermore, arsenic derivatives (mostly arsenic trioxide and arsenites, but even arsenic sulfides like As_4S_4) are much investigated for their anti-leukemia properties [13].

An important finding that came from structural studies at the solid state for several metal-nucleobase complexes was the existence of unexpected hydrogen bond type interactions as unusual base-pairing schemes. This fact had major contributions from Lippert's group [see for example: 1g,14].

Through the works carried out on some ruthenium-thiobase complexes in this laboratory in the past, it appeared that starting complexes that contain XR_3 ligands are versatile materials to obtain definite, crystalline compounds with ligands of biological interest like purines and pyrimidines. Most of the data collected in the field of Ru–XR_3 species by others and by some of us were relevant to phosphines (X = P) as co-ligands, whereas corresponding complexes with arsines and stibines were not much investigated. It was shown that thiopurines react with $[Ru(AsPh_3)_2Cl_3(CH_3OH)]$ in a way to cause the reduction of the metal center and to form bis-chelates via Ru–S^6/N^7 coordinate bonds. The complexes were characterized via spectroscopy but resisted several efforts aimed at growing single crystals suitable for X-ray diffraction studies.

On the basis of these premises, the research work on Ru–XR_3-thiobase complexes continued in this laboratory, by extending the investigations to thiopyrimidines and by paying special attention to unusual weak hydrogen bond type interactions and unusual base pairings [12b]. Here we wish to report on the synthesis, X-ray structure, spectroscopy and theoretical analysis for a Ru(II) complex with 2-thiopyrimidine-1,3 (HTPYM) (Scheme 1a) and $AsPh_3$ ligands.

2. Experimental

2.1. Materials

The compounds $RuCl_3 \cdot 3H_2O$ (Ega), $AsPh_3$ (Merck), HTPYM (Sigma) were used without any further purification. Absolute ethanol, methanol and acetonitrile were analytical grade products from Merck.

2.2. Synthesis

$[Ru^{III}(AsPh_3)_2Cl_3(CH_3OH)]$ (**1**). The compound was prepared from $RuCl_3 \cdot 3H_2O$ and $AsPh_3$ as previously described by others [15].

trans,cis,cis-[Ru($AsPh_3$)$_2$(*N,S*-TPYM)$_2$] (**2**). Fifty-six milligrams of HTPYM (0.50 mmol) was mixed with absolute ethanol (10 mL). The yellow suspension was de-aerated by bubbling ultra-pure nitrogen for 15 min and then **1** was added (217 mg, 0.40 mmol). The mixture was heated up to reflux and maintained refluxing and stirring, under nitrogen (ca. 1 bar), in the dark (3 h). A brown–red suspension was obtained, from which a small portion was collected and tested for reactivity with air. No apparent change occurred to the aerated suspension over a period of 6 h. Then, the hot suspension was filtered and the green–brown solid was taken off. The deep brown red filtrate was cooled down to room temperature and left concentrating through spontaneous solvent evaporation (in the dark). Deep-red crystals suitable for X-ray diffraction analysis formed within 24 h. They were collected, washed by using small volumes of cold absolute ethanol and then stored in air. Yield, 71 mg (30%). *Anal.* Calc. for $C_{44}H_{36}As_2N_4RuS_2$ (MW = 935.83): C, 56.47; H, 3.88; N, 5.99. Found: C, 56.07; H, 3.96; N, 6.32%. UV–Vis. ($CHCl_3$, the crystals are slightly soluble): 0.348 nm (ε, 6500 cm^{-1} mol^{-1} L), shoulder 402 nm (ε, 5800 cm^{-1} mol^{-1} L). The chloroform solution became green upon heating at 50 °C for 60 s, or at 25 °C after a few hours; the chromatographic analysis (TLC) of the green solution showed the presence of two main components: a yellow one RF 0.87 and a blue one RF 0.82. The green solution has an absorption maximum at 597 nm (estimated absorption coefficient for the blue component, 2000 cm^{-1} mol^{-1} L) and a shoulder at ca. 300 nm. IR for **2** (KBr matrix): 1534 cm^{-1} (medium m), 1480 cm^{-1} (weak w), 1436 cm^{-1} (m), 1371 cm^{-1} (strong, s), 1180 cm^{-1} (w), 1158 cm^{-1} (w), 1077 cm^{-1} (w), 1000 cm^{-1} (w), 739 cm^{-1} (m), 695 cm^{-1} (s), 668 cm^{-1} (s), 477 cm^{-1} (m). ^{1}H NMR for **2** ($CDCl_3$, freshly prepared): 7.99–7.97 ppm from TMS (1H, multiplet m, H^6), 7.62–7.60 ppm (1H, m, H^4), 7.31–7.09 ppm (15H, m, $AsPh_3$), 6.07–6.05 ppm (1H, m, H^5). ^{1}H NMR for $TPYM^-$ ($CDCl_3$): 8.27–8.23 ppm (2H, d, H^4,H^6), 6.55–6.60 ppm (1H, t, H^5).

2.3. Spectroscopy

UV–Vis. The spectra were recorded through a Lambda EZ Perkin–Elmer Spectrophotometer working under PESSW (Ver. 1.2, Rev. 3) software. The spectra were obtained by using quartz cuvettes, 1 cm path-length at 25 °C.

IR. The spectra were recorded at the solid state from KBr matrixes at 25 °C by using the Perkin–Elmer 1600 FT-IR spectrometer.

^{1}*H NMR*. The spectra were recorded by using $CDCl_3$ at 99.8 atom D%, concentrations of the compounds 0.01 mol L^{-1} for **2** and $TPYM^-$ and <0.01 mol L^{-1} for HTPYM (because of the low solubility at 22 ± 2 °C). The ^{1}H NMR spectrum of $TPYM^-$ was recorded from a $CDCl_3$ solution of HTPYM after the addition of an equivalent of pure triethylamine. The spectrometer was a Bruker Advance operating at 400 MHz.

2.4. X-ray crystallography

A well formed dark-red parallelepiped of dimensions 0.80 × 0.15 × 0.15 mm was selected under the polarizing microscope and then mounted on a glass capillary. The Siemens P4 four circle automatic diffractometer at CIADS (Centro Interdipartimentale di Analisi e Determinazioni Strutturali, University of Siena) was used for the XRD measurements. Cell dimensions were obtained through the least-squares technique from 43 high angle ($10 < 2\theta < 38°$), randomly selected, relatively strong reflections (Table 1). The analysis of intensities for groups of reflections revealed a *mmm* Laue symmetry. A total of 5001 reflections were collected at 293 ± 2 K in the range ($2.8 < 2\theta < 50°$), 4754 of which were unique and 3459 were considered observed ($I > 2\sigma(I)$). Three check reflections were measured every 97 reflections, no decaying was recorded during the data collection. The data set was corrected for Lorentz-polarization effects. The absorption correction was applied to the data set by using the ψ-scan method based on the values of four reflections.

The structure solution and refinement were performed via the direct methods and series of 12 difference-Fourier and least-squares cycles that located all the non-hydrogen atoms by using the crystallographic program SHELX-97 [16] implemented in WINGX [17].

The hydrogen atoms were set in calculated positions via the HFIX/AFIX options of SHELX-97 and they were left to ride on the atoms to which they are linked in the subsequent refinement cycles. All the non-hydrogen atoms were refined with anisotropic thermal parameters, whereas the hydrogen atoms were considered isotropically. The final conventional agreement factors were $R_1 = 0.0435$ and $wR_2 = 0.0725$ for the observed reflections.

Table 1
Selected crystallographic data for *trans,cis,cis*-[Ru($AsPh_3$)$_2$(*N,S*-TPYM)$_2$] (**2**)

Parameter	Value
Empirical formula	$C_{44}H_{36}As_2N_4RuS_2$
Formula weight	935.83
Crystal system, space group	orthorhombic, $P2_12_12_1$, # 19
Unit cell dimensions	
a (Å)	10.999(2)
b (Å)	12.536(2)
c (Å)	29.165(4)
Volume (Å^3)	4021.4(11)
Z, Calculated density (Mg m^{-3})	4, 1.546
Absorption coefficient (mm^{-1})	2.164
Reflection collected/unique [R_{int}]	5001/4754 [0.0559]
Data/restraint/parameters	3459/0/478
Final *R* indexes [$I > 2\sigma(I)$]	$R_1 = 0.0435$, $wR_2 = 0.0725$
Final *R* indexes (all data)	$R_1 = 0.0750$, $wR_2 = 0.0821$
Largest differences in peak and hole (e Å^{-3})	0.301 and −0.359

Cell measurements and data collection performed at 293 ± 2 K, through radiation Mo Kα, $\lambda = 0.71073$ Å.

The analysis of the molecular structure and molecular graphic computations were performed via PARST-97 [18] and ORTEP-3 [19]. All the software programs were implemented under the WINGX package and the Microsoft Windows-XP operating system.

2.5. Computational studies

All the computations were performed using the GUSSIAN03 package [20] implemented on IBM-SP5 clusters of computers at CINECA (Inter-University Consortium for Scientific Computation, Casalecchio di Reno, Bologna, Italy). The molecules investigated were *trans,cis,-cis*-[Ru(AsH_3)$_2$(*N,S*-TPYM)$_2$], *cis,cis,trans*-[Ru(AsH_3)$_2$(*N,S*-TPYM)$_2$], *trans,cis,cis*-[Ru($AsPh_3$)$_2$(*N,S*-TPYM)$_2$], and *cis,cis,trans*-[Ru($AsPh_3$)$_2$(*N,S*-TPYM)$_2$], (Scheme 1). The level of theory used to compute the structures was B3LYP/(Lanl2DZ, Ru; Lanl2DZ, d, As; 6-31G, CHN; 6-31G**, S) and B3LYP/(Lanl2DZ, AsRu; 6-31G, CHNS) [21] for AsH_3 and $AsPh_3$ derivatives, respectively, and the structure optimization was continued up to the threshold values implemented in GAUSSIAN03: (maximum force 0.000450 mdyne, rms – root mean square – force 0.000300 mdyne, maximum displacement 0.001800 Å, rms displacement 0.001200 Å). No negative frequency for the optimized structures were revealed from the analysis of the hessian. Molecular drawings were obtained by using the GAUSSVIEW3.0 software package [22].

3. Results and discussion

3.1. Synthesis

The reaction of [$Ru^{III}(AsPh_3)_2Cl_3(CH_3OH)$] (**1**), with 2-thiopyrimidine-1,3, HTPYM (ligand:Ru molar ratio, 1.25:1), in refluxing ethanol produced a dark-brown suspension. The red filtrate produced *trans,cis, cis*-[Ru($AsPh_3$)$_2$(*N,S*-TPYM)$_2$] (**2**), in the form of single crystals. As it happened for the reaction of **1** with 6-thiopurine (H_2TP) [23], a reduction from Ru(III) to Ru(II) occurred even with the ligand HTPYM (this work) that undergoes deprotonation followed by chelation. In case the closed shell d^6 configuration is stabilized by ligands that posses high-field donors (like S, P, As, Sb, etc.) the Ru(II) center is much stabilized even in the solution phase.

The isolation and structure characterization of *trans,cis, cis*-[Ru($AsPh_3$)$_2$(*N,S*-TPYM)$_2$] from this work (see below for structural details) is in agreement with the *equatorial* arrangement proposed for [Ru($AsPh_3$)(H_2TP)$_2$(CH_3OH)]$^{2+}$ and [Ru(DMSO)$_2$(H_2TP)$_2$]$^{2+}$ [23], (DMSO = dimethylsulfoxide) for which the very many crystal growth attempts were unsuccessful, so far. The arrangement of the $AsPh_3$ ligands is the *semi-trefoil* C_1, *Stf*-C_1, defined in Scheme 4e of Ref. [12b].

3.2. X-ray crystallography

3.2.1. The coordination sphere

The molecular structure for *trans,cis,cis*-[Ru($AsPh_3$)$_2$(*N,S*-TPYM)$_2$] (**2**), is represented in Fig. 1, whereas the selected geometrical parameters are listed in Tables 2 and 3. The coordination sphere is distorted octahedral, and the two chelating *N,S*-TPYM ligands occupy the equatorial positions and have a *cis,cis* arrangement, so that the sulfur atoms are facing each other. The strained four-member fully hetero-atom RuSCN(Ru) chelate rings cause the largest distortions from an idealized octahedron. Two arsenic atoms from the triphenylarsine ligands occupy the apical sites. The Ru–S bond distances are equal within one time the estimated standard deviation and average 2.440(2) Å, and are in perfect agreement with the corresponding value (2.451(1) Å) previously found in this laboratory for *trans,cis,cis*-[Ru(PPh_3)$_2$(*N,S*-TPYM)$_2$] (**3**) [12b]. The two apical Ru–As vectors found for **2** (lengths: 2.428(1) and 2.436(1) Å) are expectedly longer than the Ru–P vectors (2.369(1) Å) found for the corresponding PPh_3 derivative. The Ru–N bond distances (average, 2.078(6) Å) are in good agreement with the value previously found for **3** (2.063(3) Å). One can note that for both **2** and **3** the corresponding bond distances at coordination sphere have very close values; that does not happen for *cis,-cis,trans*-[Ru(PPh_3)$_2$(*N,S*-TPYM)$_2$] (**4**). The Ru–S(*trans* to N) bond distance found for [Ru(6-methyl-2-thiopyrimidinato){bis(2,2′-bipyridine)}$_2$]$^+$$ClO_4^-$ is 2.408(2) Å [24] in agreement with a lower *trans influence* by N with respect to S.

The bond angle between the apical vectors As1–Ru1–As2 (168.45(4)°) deviates significantly from the idealized value, 180°, and the deviation (11.55(4)°) is even larger

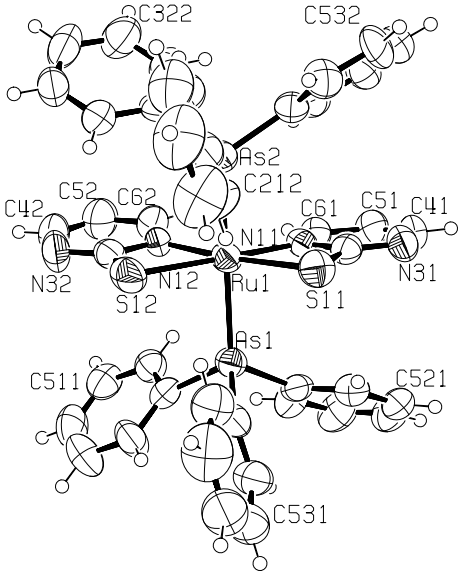

Fig. 1. Ortep style drawing of *trans,cis,cis*-[Ru($AsPh_3$)$_2$(*N,S*-TPYM)$_2$] (**2**). The labeling scheme is reported for the selected not-hydrogen atoms only, for the sake of clarity. Ellipsoids enclose 50% probability.

Table 2
Selected experimental bond distances (Å) for *trans,cis,cis*-[Ru($AsPh_3$)$_2$(*N,S*-TPYM)$_2$] (**2**)

Vector	Length
Ru1–As1	2.436(1)
Ru1–As2	2.428(1)
Ru1–S11	2.441(2)
Ru1–S12	2.438(2)
Ru1–N11	2.076(6)
Ru1–N12	2.079(6)
S11–C21	1.714(8)
S12–C22	1.699(10)
N11–C21	1.376(9)
N12–C22	1.349(9)
N11–C61	1.321(9)
N12–C62	1.345(10)
N31–C21	1.315(9)
N32–C22	1.344(11)
N31–C41	1.343(11)
N32–C42	1.325(12)
C41–C51	1.374(11)
C42–C52	1.379(13)
C51–C61	1.386(10)
C52–C62	1.375(11)
As1–C111	1.956(8)
As1–C121	1.962(7)
As1–C131	1.954(9)
As2–C112	1.971(9)
As2–C122	1.935(9)
As2–C132	1.944(8)

Table 3
Selected experimental bond angles (°) for *trans,cis,cis*-[Ru($AsPh_3$)$_2$(*N,S*-TPYM)$_2$] (**2**)

Vectors	Angle
As2–Ru1–As1	168.45(4)
N11–Ru1–S11	67.5(2)
N12–Ru1–S12	66.8(2)
S12–Ru1–S11	118.49(9)
N11–Ru1–N12	107.4(3)
N11–C21–S11	109.2(6)
N12–C22–S12	110.0(7)
N31–C21–S11	126.4(7)
N32–C22–S12	126.3(7)
N31–C21–N11	124.4(7)
N32–C22–N12	123.7(9)
C61–N11–C21	118.8(6)
C62–N12–C22	119.6(8)
C21–N31–C41	115.6(8)
C42–N32–C22	115.6(9)

than the corresponding one found for **3** (8.00(4)°). On the other hand the N–Ru–S bond angles that insist on the same $TPYM^-$ ligand average 67.2(2)° and are in perfect agreement with the value for **3** (67.51(8)°). Similarly, bond angle values in the equatorial plane for N11–Ru1–N12, 107.4(3)°, and S12–Ru1–S11, 118.49(9)° are in perfect agreement with the corresponding ones found for **3** (106.1(1)° and 119.12(4)°, respectively).

The metal atom lies on the least-squares plane defined by the four donor atoms from the $TPYM^-$ ligands.

3.2.2. The $TPYM^-$ ligands

The coordination mode shown by $TPYM^-$ ligands for **2** is the common one represented as **VIII** in Scheme 1a in Ref. [12b]. The S–C bond distances average 1.706(8) Å in agreement with an intermediate character between the thione and thiol types. The N1x–C2x vectors included in the coordination rings have lengths that average 1.362(9) Å, whereas the other six N–C bond lengths average 1.332(9) Å. Even though the difference between the two sets of N–C bond lengths is ca. within twice the esd, a lengthening effect on N1–C2 bonds by the coordination is reasonable. Distances relevant to the C–C bonds have normal values and average 1.379(10) Å.

As expected, the (Ru)N1–C–S(Ru) bond angles (average 109.6(6)°) are much smaller than the N3–C–S(Ru) angles (126.3(7)°) in agreement with a strong *N,S* chelation by $TPYM^-$. It has to be noted that the sulfur atoms deviate significantly from the least-squares plane defined by the endo-cyclic atoms (0.135(2) and 0.069(2) Å). The two least-squares planes defined by endo-cyclic atoms from $TPYM^-$ are twisted by 8.9(3)°. The metal coordination to N1 reflects in a significant widening of the two C–N1–C bond angles (119.2(7)°) with respect to the C–N3–C ones (115.6(8)°).

Intra-molecular contacts that involve $TPYM^-$ ligands are of hydrogen bond type and $\pi\cdots\pi$ stacking type.

Note worthy, both the sulfur atoms are hydrogen acceptors from phenyl rings, namely C212–H···S11 (C···S, 3.50(1) Å; Ĥ, 133(1)°) and C231–H···S12 (C···S, 3.63(1) Å; Ĥ, 136(1)°); this datum has to be compared to the bending of the Ru–As vectors towards the sulfur region.

Stacking interaction occurs between the N11/C61 $TPYM^-$ system and the C121/C621 phenyl-ring; in fact, C21···C621 and N11···C121 contact distances are 3.33(1) and 3.39(1) Å, respectively, and the dihedral angle between the two least-squares planes is 27.2(3)°. A similar interaction occurs between the N12/C62 $TPYM^-$ and the C122/C622 ring systems for which the dihedral angle between the least-squares planes is 30.3(3)° and short contact distances are C22···C622 (3.28(1)Å), N12···C122 (3.40(1) Å) and S12···C622 (3.61(1) Å).

3.2.3. $AsPh_3$ ligand

The As–C bond distances average 1.954(13) Å and range 1.935(9)–1.971(9) Å. The values compare well with those reported for *trans*-[$Rh^I(AsPh_3)_2Cl(CO)$] [25]. Corresponding values found for P–C bonds in *trans,cis,cis*-[Ru(PPh_3)$_2$(*N,S*-TPYM)$_2$] are 1.833(4) Å, range 1.828(4)–1.837(4) Å. The analysis of the bond angles is as follows: Ru–As–C, average 116.4° (esds from the six values 1.6°), range 113.6–117.3(2)°; C–As–C, average 101.7(18)°, range 99.6(4)–104.2(4)°. Corresponding values for the Ru–P–C and C–P–C angles in *trans,cis,cis*-[Ru(PPh_3)$_2$(*N,S*-TPYM)$_2$] are average 113.5(23)°, range 111.4(1)–115.9(1)°, and average 105.1(45)°, range 101.0(2)–109.9(2)°. The data show that C–As–C angles are smaller than the C–P–C ones in agree-

ment with a smaller cone angle for $AsPh_3$ than for PPh_3. The examination of the Ru–S bond distances for *trans,cis,cis*-[$Ru(XPh_3)_2$(*N,S*-TPYM)$_2$] (reported above) suggests a larger *cis influence* for X = P when compared to X = As.

3.2.4. Inter-molecular contacts

Some C–H···N hydrogen-bond type interactions occur between C–H functions and the non-coordinate nitrogen atoms. For example, C232 and N31 related by a screw-axis parallel to **a** cell edge have contact parameters: C($x + 1/2$, $-y + 1/2$, $-z$)···N, 3.58(1) Å, and Ĥ, 148(1)°; C411 and N32 related by a screw-axis parallel to **b** cell edge have parameters C($-x$, $+y + 1/2$, $-z + 1/2$)···N, 3.78(1) Å and Ĥ, 138(1)°. On examining possible base pairings, it appears that C51 and S11 have distances and angles as follows: C($x + 1/2$, $-y + 1/2$, $-z$)···S, 3.65(1) Å and Ĥ, 113(1)°, whereas C61 and N31 from the same unit have C···N, 3.72(1) Å and Ĥ, 119(1)°. Thus, the arrangement of the two bases is such to look like a base pairing (Fig. 2a), even though the linkage is reasonably weak because the two pyrimidine rings do not lie on the same plane (Fig. 2b). The N12/C62 pyrimidine system is not involved in such a type of base···base interaction. Instead the S12 atom is hydrogen acceptor from C412($-x + 1$, $+y - 1/2$, $-z + 1/2$) (C···S, 3.58(1) Å; Ĥ, 138(1)°) and from C512($-x + 1$, $+y - 1/2$, $-z + 1/2$) (C···S, 3.79(1) Å; Ĥ, 117(1)°), whereas the N32 atom is hydrogen acceptor from C422($-x$, $+y - 1/2$, $-z + 1/2$) (C···S, 3.48(1) Å; Ĥ, 113(1)°) and from C522($-x$, $+y - 1/2$, $-z + 1/2$) (C···S, 3.51(1) Å; Ĥ, 112(1)°), and from C411($-x$, $+y + 1/2$, $-z + 1/2$) (C···S, 3.78(1) Å; Ĥ, 138(1)°) (Fig. 3). It is worthy of note that weak C–H···N, C–H···S and C–H···Cl hydrogen bond type interactions play important roles in coordination and organometallic compounds, as previously shown from this laboratory and from others [26–30].

3.2.5. Spectroscopy

UV–Vis. The spectrum of a freshly prepared solution of **2** in $CHCl_3$ (4.3×10^{-5} M) is reported in Fig. 4. The

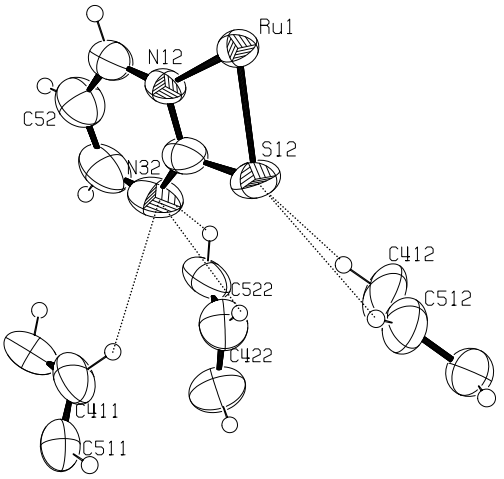

Fig. 3. The diagram shows selected intra-molecular hydrogen bond type interactions that involve a $TPYM^-$ ligand.

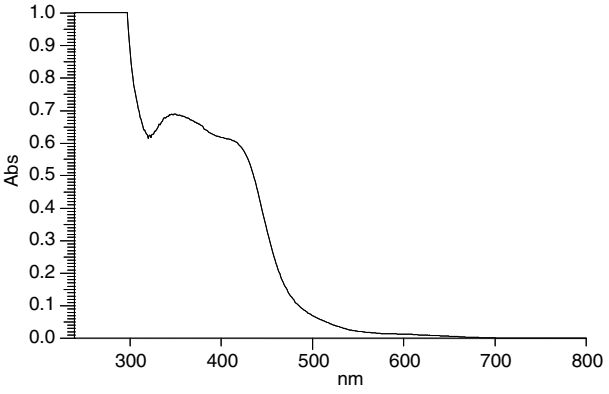

Fig. 4. Absorption UV–Vis spectrum for *trans,cis,cis*-[$Ru(AsPh_3)_2$(*N,S*-TPYM)$_2$] (4.3×10^{-5} M) in chloroform (fresh solution).

absorption band at 348 nm (ε, 16 000 cm^{-1} mol^{-1} L) and the shoulder at 402 nm (ε, 14 300 cm^{-1} mol^{-1} L) compare well with the values previously found for *trans,cis,cis*-[$Ru(PPh_3)_2$(*N,S*-TPYM)$_2$] and show a shift towards lower energy for the arsine derivative. The absorptions in the

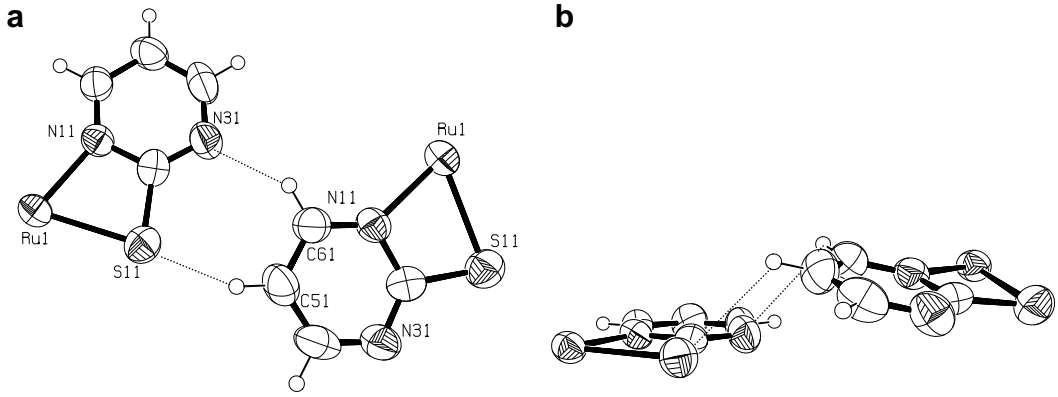

Fig. 2. The diagram shows the way two thiopyrimidine ligands are arranged in a pairing-type fashion through weak C–H···S and C–H···N interactions: (a) the view is almost perpendicular to the least-squares planes that are defined by the endo-cyclic atoms; (b) the view is almost parallel to the same planes. The Ru atom and the atoms from $TPYM^-$ only are pictured for the sake of clarity.

UVA region are assigned to ligand ($TPYM^-$)-to-metal charge transfer on the basis of computations reported in [12b]. The absorption band at λ_{max} 597 nm recorded from the solution of **2** in chloroform after 24 h from the preparation is responsible for the green color of the solution. Chromatographic analysis of the solution (TLC, reverse phase C18, eluent CH_3CN) revealed two components: R_F 0.88 (yellow fraction) and R_F 0.82 (blue fraction). The molar absorbance was roughly estimated to be ca. 2000 cm^{-1} mol^{-1} L. These data compare well with those for *trans,cis,cis*-$[Ru^{III}(PPh_3)_2(\underline{N,S}\text{-}TPYM)_2]^+$ obtained via electrochemical oxidation [12b].

^1H NMR. The three signals relevant to the (C)H protons from TPYM anions for **2** in $CDCl_3$ are in agreement with a C_s symmetry at metal (free rotation of $AsPh_3$ around Ru–As; 22 ± 2 °C). As expected, the local C_{2v} symmetry for free $TPYM^-$ no longer exists for the ligand in **2**. The chemical shift values for **2** (average 7.98, 7.61, 6.06 ppm for H^6, H^4 and H^5, respectively) are in good agreement with corresponding values previously found for other compounds, from here $[Ru^{II}(PPh_3)_2(\underline{N,S}\text{-}TPYM)_2]$ [12b], and by other workers [Pd($\underline{C^1,N}$-2-(dimethylaminomethyl)phenyl)(μ-$\underline{N,S}$-TPYM)]$_2$ [31] and $[M(CF_3\text{-}\underline{N,S}\text{-}TPYM)_2(PPh_3)_2]$ (M = Ru, Os) [32].

Interestingly, the chemical shifts for the signals from (C)H protons of $TPYM^-$ undergo a net up-field change upon metal chelation via N^1 and $(C^2)S$ atoms. The effect is ca. 0.27, 0.64 and 0.57 ppm for H^6, H^4 and H^5, respectively.

3.3. Computational studies

3.3.1. Structures

The structure for the model molecule *trans,cis,cis*-$[Ru(AsH_3)_2(\underline{N,S}\text{-}TPYM)_2]$ as optimized through the density functional methods (see Section 2.5) is represented in Fig. 5a, whereas the selected geometrical parameters are listed in Table 4. The computed Ru–As bond distances 2.455 Å are very close to the experimental value found for *trans,cis,cis*-$[Ru(AsPh_3)_2(\underline{N,S}\text{-}TPYM)_2]$ (average, 2.432(1) Å). A similar good agreement is found for Ru–N bond distances: computed 2.118 Å, experimental 2.078(6) Å, whereas the computed value for the corresponding PH_3 derivative was 2.113 Å. The computed Ru–S bond distances (2.516 Å) compare well with the experimental values (average found Ru–S distance, 2.440(2) Å). As expected, the choice of the basis set for the soft atoms is very important in simulating this type

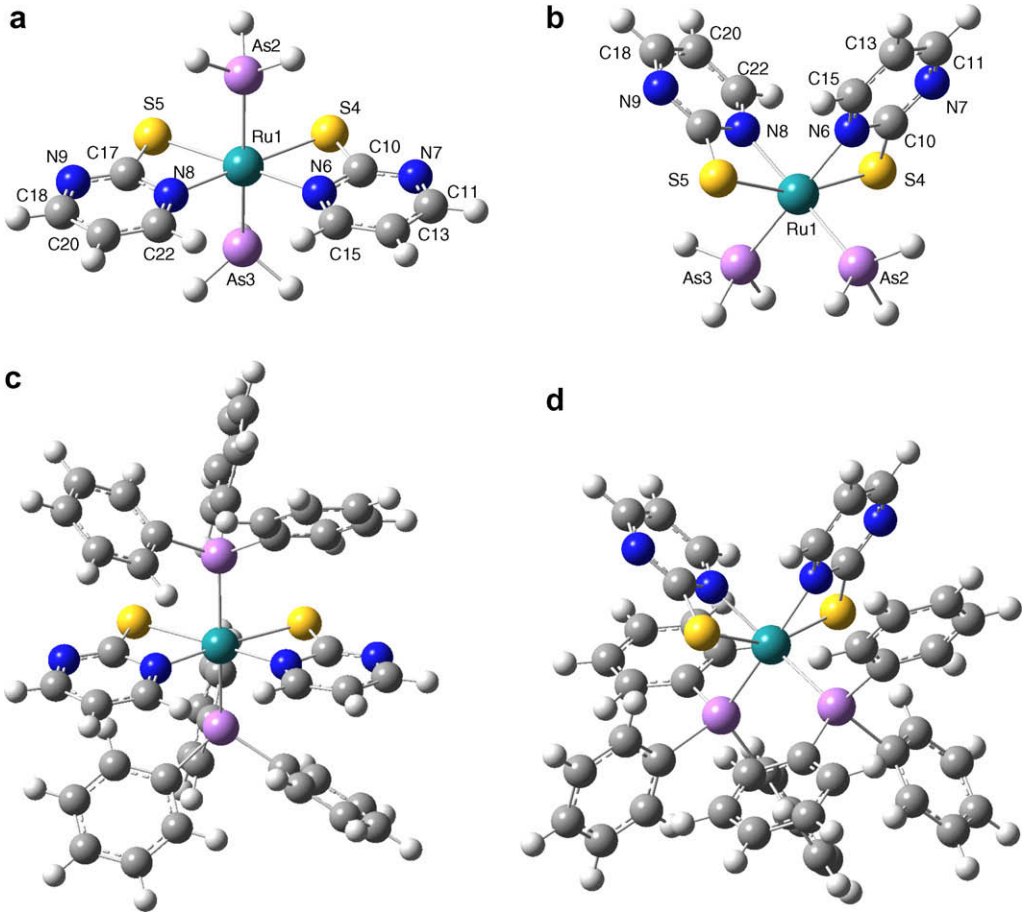

Fig. 5. GaussView style drawing for the optimized molecules: (a) *trans,cis,cis*-$[Ru(AsH_3)_2(\underline{N,S}\text{-}TPYM)_2]$; (b) *cis,cis,trans*-$[Ru(AsH_3)_2(\underline{N,S}\text{-}TPYM)_2]$; (c) *trans,cis,cis*-$[Ru(AsPh_3)_2(\underline{N,S}\text{-}TPYM)_2]$; (d) *cis,cis,trans*-$[Ru(AsPh_3)_2(\underline{N,S}\text{-}TPYM)_2]$. The computations have been performed via DFT-B3LYP methods (see text for basis sets and Table 4 for the selected computed geometrical parameters).

Table 4
Selected computed bond distances (Å) and angles (°) for *trans,cis,cis*-[Ru(AsH$_3$)$_2$(*N,S*-TPYM)$_2$] (tcc), and *cis,cis,trans*-[Ru(AsH$_3$)$_2$(*N,S*-TPYM)$_2$] (cct) model isomers

Vector	Length	
	tcc	cct
Ru1–As2/3	2.455	2.445
Ru1–S4/5	2.516	2.514
Ru1–N6/8	2.118	2.101
S4/5–C10/17	1.731	1.736
N6/8–C10/17	1.399	1.393
N6/8–C15/22	1.353	1.350
N7/9–C10/17	1.358	1.358
N7/9–C11/18	1.354	1.355
C11/18–C13/20	1.413	1.412
C13/20–C15/22	1.405	1.406
As2/3–H	1.525	1.524
As2/3–H	1.516	
Vectors	Angle	
As2–Ru1–As3	168.8	93.3
N6/8–Ru1–S4/5	67.0	67.3
S4–Ru–S5	115.3	158.7
N6–Ru1–N8	110.8	87.0
N6/8–C10/17–S4/5	110.4	110.5
N7/9–	126.6	126.9
N6/8–C10/C17–N7/9	123.0	122.6
C10/17–N6/8–C15/C22	118.8	119.9
C10/17–N7/9–C11/18	117.4	117.1

The computational method (see text) was the hybrid density functional B3LYP and the basis set was: (Lanl2DZ, Ru; Lanl2DZ, d, As; 6-31G, CHN; 6-31 G**, S). Average values are reported. The labeling of the atom is that shown in Fig. 5.

of complexes. In fact, the same model structure as optimized by using the 6-31G type functions for AsCHNS atoms (Lanl2DZ for Ru) has longer Ru–As,S bond distances: computed Ru–As, and Ru–S are 2.478, and 2.562 Å. As a consequence of the increased coordination distances for the heavier donors, the computed Ru–N distances decrease and average 2.105 Å.

On the basis of this analysis, the mixed basis set that has more expanded functions for As and S only, and 6-31G-type functions for CHN atoms were considered reliable for estimating bond lengths.

The computed bond angles at metal center reproduce very well the experimental values, for example S–Ru–N chelation angles are 67.0°, whereas the average value for the solid state structure is 67.2(2)°.

The same methodology was applied to compute the structure of *cis,cis,trans*-[Ru(AsH$_3$)$_2$(*N,S*-TPYM)$_2$] (Fig. 5b), that has been selected as model for the corresponding triphenylarsine derivative.

The computed Ru–As and –S bond distances for *cis,-cis,trans* isomer do not differ appreciably from those relevant to the corresponding ones for *trans,cis,cis*. However, the Ru–N bond distances for *cis,cis,trans* are shorter by 0.017 Å with respect to those for *trans,cis,cis*; thus the chelation of Ru by TPYM$^-$ seems to be stronger in the case of the *cis,cis,trans* isomer when compared to *trans,cis,cis*. This hypothesis is confirmed by the comparative analysis of the computed bond angles at metal for the two isomers. The angles for *trans,cis,cis* have larger deviations from canonical idealized values of 90° and 180° than for *cis,cis,-trans*: N–Ru–N deviates by 20.8° in *trans,cis,cis* and 3° in *cis,cis,trans*, As–Ru–As deviates by 11.2° and 3.3° in *trans,cis,cis* and *cis,cis,trans*, respectively, S–Ru–S deviates by 25.3° in *trans,cis,cis* and by 21.3° in *cis,cis,trans*. From this analysis it is reasonable to predict that the *cis,cis,trans* isomer is more stable than the *trans,cis,cis* one (see section 3.3.2).

On comparing the differences between the computed Ru–N bond distances for complex molecules that contain PH_3 and AsH_3 it is evident that a larger *trans influence* by phosphines occurs [25].

The structural parameters for the chelating TPYM$^-$ anions are the same within each isomer and do not deviate much on passing from *trans,cis,cis* to *cis,cis,trans*. The S–C bond is slightly longer for *cis,cis,trans* than for *trans,cis,cis* (by 0.005 Å), in agreement with a stronger chelation to the metal for *cis,cis,trans*.

3.3.2. Energy and modeling of the base-pairing type interaction

The total electronic energy is −657.44121 and −657.44903 hartrees for *trans,cis,cis*-[Ru(AsH$_3$)$_2$(*N,S*-TPYM)$_2$] and *cis,cis,trans*-[Ru(AsH$_3$)$_2$(*N,S*-TPYM)$_2$] isomers, respectively, showing that the order of stability predicted from the structural strains commented just above was correct. The difference corresponds to 4.907 kcal mol^{-1}, and it is large enough to suggest a preponderance of the *cis,cis,trans* isomer compared to *trans,cis,cis* in the mother mixtures, provided that the starting complex contains the AsR_3 ligands in both the *cis* and *trans* arrangements (or provided that the *cis*/*trans* inter-conversion has a low energy barrier). It has to be recalled that the reaction of [RuCl$_2$(PPh$_3$)$_3$] with HTPYM produces the corresponding *cis,cis,trans*-[Ru(PPh$_3$)$_2$(*N,S*-TPYM)$_2$] as the major product and *trans,cis,cis*-[Ru(PPh$_3$)$_2$(*N,S*-TPYM)$_2$] in a lower yield. In fact, [RuCl$_2$(PPh$_3$)$_3$] has a pseudo-trigonal bipyramidal arrangement with two chloride and a phosphorous atom in the equatorial plane and two triphenylphosphine ligands almost *trans* each to other [33]. In this latter case the coordination arrangement of the starting material and the higher *trans* influence of P over As are such to allow the formation of the two isomers at a molar ratio that reflects the relative stability.

On the contrary, in the case of the present work the starting compound has a *trans* arrangement of the arsenic atoms, whereas the more labile donors, alcohol oxygen and chloride anions occupy the equatorial plane. That arrangement seems to allow first the formation of the two stable chelate systems in the equatorial plane and thus the *trans,cis,cis* isomer; the subsequent isomerization to *cis,cis,trans* albeit favored by a higher stability of *cis,cis,-trans* over *trans,cis,cis* is not favored because of high energy barriers. A similar behavior was found for a 6-thiopurine

H_2TP derivative obtained from the reaction of *trans*-$[Ru(AsPh_3)_2Cl_3(CH_3OH)]$ with H_2TP. In the case of bulkier H_2TP (when compared to $TPYM^-$) the bis-chelate allows the presence of just one $AsPh_3$ and the formation of $[Ru(AsPh_3)(\underline{N,S}\text{-}H_2TP)_2(CH_3OH)]Cl_2$ [23] instead of $[Ru(AsPh_3)_2(\underline{N,S}\text{-}H_2TP)_2]Cl_2$. Even for the H_2TP derivative the arrangement of the two chelating thiobases is equatorial.

The computed total electronic energies for *trans,cis,cis*- and *cis,cis,trans*-$[Ru(AsPh_3)_2(\underline{N,S}\text{-}TPYM)_2]$ performed at the B3LYP/(Lanl2DZ, AsRu; 6-31G, CHNS) level have the same trend as that presented above for the AsH_3 derivatives, the *cis,cis,trans* isomer being more stable by 4.060 kcal mol^{-1} than the *trans,cis,cis* one.

As regards the thiopyrimidine-pairing type interaction mentioned above (Section 3.2.4), it has to be recalled that previous computations relevant to the pairing for $\{cis\text{-}[(NH_3)_2Pt(HTP\text{-}\ H^1)\cdots(H_2TP)\}^+$ aggregate assisted by a $N\text{–}H\cdots N^-$ and a $C\text{–}H\cdots S$ interactions, estimated an adduct formation energy of ca. −7 kcal mol^{-1} [28]. It is reasonable to assume that the computed energy contribution for pairing interaction found in the structure of **2** (see above) can be approximated roughly to that magnitude for the gas phase and without any correction for the basis set superposition error (BSSE). Furthermore, the paired (Ru)$TPYM^-$ moieties for **2** are not coplanar (Fig. 2b); this fact should decrease the pairing energy.

The computed pairing energy for a non-metal bound {$TPYM^-$...HTPYM} planar system (the two bases linked via $C\text{–}H\cdots S$ and $C\text{–}H\cdots N$ and kept constrained to move in the plane) is ca. −19 kcal in the gas phase at the B3LYP/(6-31G**, CHNS) level, without any correction for BSSE. The optimization did not meet the convergence criteria implemented in GAUSSIAN03 and was halted when three out of four criteria were satisfied. The maximum displacement item being relatively high, 0.020298. The selected contact distances for the partially optimized aggregate ($H^5\cdots S$ and $H^6\cdots N$, 2.588 and 2.253 Å) are significantly shorter than experimental value for **2** (3.193 and 3.175 Å), thus that the estimated pairing energy for planar {$TPYM^-$...HTPYM} is undoubtedly higher than the value for the pairing of two complex molecules. The pairing interaction seems to be electrostatic-type in **2**; the sum of Van der Waals radii for H and S, and H and N atoms being 3.00–3.25 Å, and 2.75–3.00 Å, respectively [34,35]. The selected Mulliken atomic charges computed for {$TPYM^-$...HTPYM} planar system are $S(-0.49\ e)\cdots H^5(0.17\ e)$ and $N^3(-0.45\ e)\cdots H^6(0.17\ e)$.

3.3.3. Vibration frequencies

The analysis of the vibrations for *trans,cis,cis*-$[Ru(AsH_3)_2(\underline{N,S}\text{-}TPYM)_2]$ shows that the symmetric stretching of the two Ru–As bond has a computed frequency of 182.09 cm^{-1} (force constant, 0.3849 mdyn $Å^{-1}$) and is predicted to be weak (IR intensity, 0.3002 km mol^{-1}). The corresponding asymmetric Ru–As stretching vibrations (associated with oscillation for S atoms out of the $TPYM^-$ plane) have values: 201.39 cm^{-1} (0.2058 mdyn $Å^{-1}$, 1.9169 km mol^{-1}), and 262.68 cm^{-1} (0.4389 mdyn $Å^{-1}$, 0.3494 km mol^{-1}). The asymmetric Ru–S stretching vibrations associated with N–C–S in plane vibrations are mostly defined by the computed frequence 292.5 cm^{-1} (1.073 mdyn $Å^{-1}$, 10.10 km mol^{-1}). Computed vibrations that have contributions from complex Ru–N stretching and N–C–S bending motions have the values: 393.9 cm^{-1} (0.624 mdyn $Å^{-1}$, 5.254 km mol^{-1}). Computed infrared absorption that have contributions from C–S stretching have frequencies: 472.5 cm^{-1} (1.754 mdyn $Å^{-1}$, 8.382 km mol^{-1}), 997.7 cm^{-1} (5.131 mdyn $Å^{-1}$, 41.289 km mol^{-1}), 1173.2 cm^{-1} (1.813 mdyn $Å^{-1}$, 38.513 km mol^{-1}), and 1255.9 cm^{-1} (4.203 mdyn $Å^{-1}$, 59.341 km mol^{-1}). Intense computed absorption effects occur at 1407.0 cm^{-1}, combinations of C–N stretching and H–C–N bending in $TPYM^-$ plane, 1586.7 cm^{-1}, combinations of C–N and C–C stretching and H–C–N bending in plane, 2208.8 cm^{-1}, and 220.4 cm^{-1}, As–H stretching motions.

As regards the *cis,cis,trans* derivative, the computed IR spectrum is similar to that for the *trans,cis,cis* isomer both for the frequencies and intensities. For example, computed effects that come from C–S stretching motions are at 470.7 cm^{-1}, 1004.3 cm^{-1}, 1180.3 cm^{-1}, 1256.9 cm^{-1}. As a consequence, infrared spectroscopy is not a suitable technique to discriminate between the two isomers.

The comparative analysis between the computed IR spectrum for *trans,cis,cis*-$[Ru(AsH_3)_2(\underline{N,S}\text{-}TPYM)_2]$ and the experimental data found at the solid state for **2**, in the spectral region relevant to vibrations that involve $TPYM^-$, shows a remarkable agreement (see Section 2.2).

4. Conclusion

In conclusion the work produced the new *trans,cis,cis*-$[Ru(AsPh_3)_2(\underline{N,S}\text{-}TPYM)_2]$ crystalline compound that might be of interest for testing as an anti-cancer drug. The X-ray diffraction analysis and the spectroscopy studies confirm that the solid state and solution phase structures are the same. The compound is stable for years at the solid state in the air atmosphere, but might easily decompose when in solution. Studies devoted to investigate the nature of other products from the preparative reaction, and to draw light on the mechanism for the reactivity in solution are in progress in this laboratory. Preliminary results (via HPLC) show that in chloroform, acetonitrile and methanol solution, the first step of the reaction cascade is the dissociation of $Ru\text{–}AsPh_3$ bond(s).

The *cis,cis,trans*-$[Ru(AsPh_3)_2(\underline{N,S}\text{-}TPYM)_2]$ isomer is predictably more stable than the corresponding *trans,cis,-cis*, as shown via density functional computational tools; nevertheless, it could not be isolated at the solid state nor detected as a major component via spectroscopy or chromatography so far. The coordination arrangement of the starting compound **1** that has two triphenylarsine ligands *trans* to each other, or the different solubility in alcoholic media of the two possible isomers, makes the isolation of

trans,cis,cis at the solid state easier even though its overall stability is lower.

Finally, the work revealed a tendency for two {Ru(*N,S*-TPYM)} coordination systems to pair via unusual C^5–H···S and C^6–H···N^3 interactions.

Acknowledgements

The authors are indebted to Prof. Dr. Bernhard Lippert for having shown us the beauty and the importance of metal-nucleobase compounds. His leading researches in the field of bio-inorganic chemistry sustained the enthusiasm of the workers from this group during the years.

The authors thank University of Siena for funding through the PAR (Piano di Ateneo per la Ricerca) and Ministero dell'Università e della Ricerca Scientifica e Tecnologica (MURST, Rome) through PRIN (Progetto di Rilevante Interesse Nazionale) year 2004 (Contract No. 2004032118). Thanks are also expressed to Dr. Francesco Berrettini for the X-ray diffraction data collection at CIADS (Centro Interdipartimentale di Analisi e Determinazioni Strutturali, University of Siena).

Appendix A. Supplementary material

CCDC 643223 contains the supplementary crystallographic data for *trans,cis,cis*-[$Ru(AsPh_3)_2$(*N,S*-TPYM)$_2$]. These data can be obtained free of charge via http://www.ccdc.cam.ac.uk/conts/retrieving.html, or from the Cambridge Crystallographic Data Centre, 12 Union Road, Cambridge CB2 1EZ, UK; fax: (+44) 1223-336-033; or e-mail: deposit@ccdc.cam.ac.uk.

Tables of atomic coordinates of fully optimized complex molecules *trans,cis,cis*- and *cis,cis,trans*-[$Ru(AsH_3)_2$(*N,S*-TPYM)$_2$], and *trans,cis,cis*- and *cis,cis,trans*-[$Ru(AsPh_3)_2$-(*N,S*-TPYM)$_2$], and ligand molecules HTPYM and $TPYM^-$, and the partially optimized adduct {$TPYM^-$... HTPYM} (seven Tables). Supplementary data associated with this article can be found, in the online version, at doi:10.1016/j.ica.2007.07.026.

References

[1] (a) D. Gupta, M. Huelsekopf, M. Morell Cerdà, R. Ludwig, B. Lippert, Inorg. Chem. 43 (2004) 3386;
(b) R. Griesser, G. Kampf, L.E. Kapinos, S. Komeda, B. Lippert, J. Reedijk, H. Sigel, Inorg. Chem. 42 (2003) 32;
(c) M. Willermann, C. Mulcahy, R.K.O. Sigel, M. Morell Cerdà, E. Freisinger, P.J. Sanz Miguel, M. Roitzsch, B. Lippert, Inorg. Chem. 45 (2006) 2093;
(d) D. Gupta, M. Roitzsch, B. Lippert, Inorg. Chim. Acta 360 (2007) 2379;
(e) E. Yareth Biviá-Castro, M. Roitzsch, D. Gupta, B. Lippert, Inorg. Chim. Acta 358 (2005) 2395;
(f)B. Lippert (Ed.), Cisplatin: Chemistry and Biochemistry of a Leading Anticancer Drug, Wiley, 1999;
(g) B. Lippert, Alteration of Nucleobase pK_a Values Upon Metal Coordination: Origins and Consequences, in: K.D. Karlin (Ed.), Prog. Inorg. Chem., Vol. 54, 2005 (Chapter 6th).

[2] (a) A. Dobrov, V.B. Arion, N. Kandler, W. Ginzinger, M.A. Jakupec, A. Rufińska, N. Graf von Keyserlingk, M. Galanski, C. Kowol, B.K. Keppler, Inorg. Chem. 45 (2006) 1945;
(b) M.A. Jakupec, E. Reisner, A. Eichinger, M. Pongratz, V.B. Arion, M. Galanski, C.G. Hartinger, B.K. Keppler, J. Med. Chem. 48 (2005) 2831;
(c) S.S. Aleksenko, C.G. Hartinger, O. Semenova, K. Meelich, A.R. Timerbaev, B.K. Keppler, J. Chromatogr. A 1155 (2007) 218.

[3] (a) D. Bhattacharyya, P.A. Marzilli, L.G. Marzilli, Inorg. Chem. 44 (2005) 7644;
(b) M. Carlone, L.G. Marzilli, G. Natile, Inorg. Chem. 43 (2004) 584.

[4] R. Prabhakaran, R. Huang, K. Natarajan, Inorg. Chim. Acta 359 (2006) 3359.

[5] (a) A. Magistrato, P. Ruggerone, K. Spiegel, P. Carloni, J. Reedijk, J. Phys. Chem. B 110 (2006) 3604;
(b) K. Karidi, A. Garoufis, N. Hadjiliadis, M. Lutz, A. Spek, J. Reedijk, Inorg. Chem. 45 (2006) 10282.

[6] T.H. Scheuermann, C. Keeler, M.E. Hodsdon, Biochemistry 43 (2004) 12198.

[7] S. Shigeta, S. Mori, F. Watanabe, K. Takahashi, T. Nagata, N. Koike, T. Wakayama, M. Saneyoshi, Antivir. Chem. Chemother. 13 (2002) 67.

[8] (a) A. Massey, Y.Z. Xu, P. Karran, DNA Repair 1 (2002) 275;
(b) A. Massey, Y.Z. Xu, P. Karran, Curr. Biol. 11 (2001) 1142;
(c) P. Karran, Br. Med. Bull. 79–80 (2006) 153.

[9] A. Teml, E. Scheffeler, K.R. Herrlinger, U. Klotz, M. Schwab, Clin. Pharmacokint. 46 (2007) 187.

[10] (a) T.M. Hunter, I.W. McNae, X. Liang, J. Bella, S. Parsons, M.D. Walkinshaw, P.J. Sadler, Proc. Natl. Acad. Sci. USA 102 (2005) 2288;
(b) T.M. Hunter, S.J. Paisey, H.S. Park, L. Cleghorn, A. Parkin, S. Parsons, P.J. Sadler, J. Inorg. Biochem. 98 (2004) 713.

[11] (a) R.A. Alderden, H.R. Mellor, S. Modok, T.W. Hambley, R. Callaghan, Biochem. Pharmacol. 71 (2006) 1136;
(b) C.D. Dillon, T.W. Hambley, B.J. Kennedy, P.A. Lay, J.E. Weder, Q. Zhou, Met. Ions Bion. Syst. 41 (2004) 253.

[12] (a) G. Tamasi, L. Chiasserini, L. Savini, A. Sega, R. Cini, J. Inorg. Biochem. 99 (2005) 1347;
(b) R. Cini, G. Tamasi, S. Defazio, M. Corsini, P. Zanello, L. Messori, G. Marcon, F. Piccioli, P. Orioli, Inorg. Chem. 42 (2003) 8038.

[13] T. Kumagai, L.Y. Shih, S.V. Hughes, J.C. Desmond, J. O'Kelly, M. Hewison, H.P. Koeffler, Cancer Res. 65 (2005) 2488.

[14] R.K.O. Sigel, E. Freisinger, S. Metzeger, B. Lippert, J. Am. Chem. Soc. 120 (1998) 12000.

[15] T.A. Stephenson, G. Wilkinson, J. Inorg. Nucl. Chem. 28 (1966) 945.

[16] G.M. Sheldrick, SHELXS/L-97 Programs for the Solution/Refinement of Crystal Structures, University of Göttingen, Göttingen, Germany, 1997.

[17] (a) L.J. Farrugia, WINGX an Integrated System of Windows Programs for the Solution, Refinement and Analysis of Single Crystal X-Ray Diffraction Data, version 1.64.05, University of Glasgow, Glasgow, UK, 1999–2003;
(b) L.J. Farrugia, J. Appl. Crystallogr. 32 (1999) 837.

[18] M. Nardelli, PARST-97, A System of Computer Routines for Calculating Molecular Parameters from Results of Crystal Structure Analyses, University of Parma, Parma, Italy, 1997.

[19] C.K. Johnson, M.N. Burnett, ORTEP-3 for Windows, Oak Ridge National Laboratory, 1998. 32-bit Implementation by L.J. Farrugia, University of Glasgow, Glasgow, UK, 1999.

[20] M.J. Frisch, G.W. Trucks, H.B. Schlegel, G.E. Scuseria, M.A. Robb, J.R. Cheeseman, J.A. Montgomery Jr., T. Vreven, K.N. Kudin, J.C. Burant, J.M. Millam, S.S. Iyengar, J. Tomasi, V. Barone, B. Mennucci, M. Cossi, G. Scalmani, N. Rega, G.A. Petersson, H. Nakatsuji, M. Hada, M. Ehara, K. Toyota, R. Fukuda, J. Hasegawa, M. Ishida, T. Nakajima, Y. Honda, O. Kitao, H. Nakai, M. Klene, X. Li, J.E. Knox, H.P. Hratchian, J.B. Cross, V. Bakken, C. Adamo, J. Jaramillo, R. Gomperts, R.E. Stratmann, O. Yazyev, A.J. Austin, R. Cammi, C. Pomelli, J.W. Ochterski, P.Y. Ayala, K. Morokuma, G.A.

Voth, P. Salvador, J.J. Dannenberg, V.G. Zakrzewski, S. Dapprich, A.D. Daniels, M.C. Strain, O. Farkas, D.K. Malick, A.D. Rabuck, K. Raghavachari, J.B. Foresman, J.V. Ortiz, Q. Cui, A.G. Baboul, S. Clifford, J. Cioslowski, B.B. Stefanov, G. Liu, A. Liashenko, P. Piskorz, I. Komaromi, R.L. Martin, D.J. Fox, T. Keith, M.A. Al-Laham, C.Y. Peng, A. Nanayakkara, M. Challacombe, P.M.W. Gill, B. Johnson, W. Chen, M.W. Wong, C. Gonzalez, J.A. Pople, GAUSSIAN03, Revision D.02, Gaussian Inc., Wallingford, CT, 2004.

[21] (a) A. Frisch, M.J. Frisch, GAUSSIAN98, User's Reference, second ed., Gaussian, Inc., Carnegie Office Park, Building 6, Pittsburgh, PA 15106, 1998;
(b) C.E. Check, T.O. Faust, J.M. Bailey, B.J. Wright, T.M. Gilbert, L.S. Sunderlin, J. Phys. Chem. A 105 (2001) 1811.

[22] GaussView3.0, Gaussian Inc., Carneige Office Park-Bldg 6, Pittsburg, PA 15106, USA.

[23] C. Pifferi, R. Cini, J. Chem. Soc., Dalton Trans. (1998) 2679.

[24] K. Yamanari, T. Nozaki, A. Fuyuhiro, Y. Kushi, S. Kaizaki, J. Chem. Soc., Dalton Trans. (1996) 2851.

[25] S. Otto, A. Roodt, Inorg. Chim. Acta 357 (2004) 1.

[26] R. Cini, C. Bellucci, G. Tamasi, M. Corsini, M. Fontani, P. Zanello, Inorg. Chim. Acta 339 (2002) 89.

[27] S. Defazio, G. Tamasi, R. Cini, Compt. Rend. Chim. 8 (2005) 1584.

[28] G. Tamasi, F. Botta, R. Cini, J. Mol. Struct.: Theochem. 766 (2006) 61.

[29] H.-B. Zhu, Z.-L. Chu, D.-H. Hu, W. Huang, S.-H. Gou, Inorg. Chem. Commun. 10 (2007) 362.

[30] W.-J. Shi, L. Hou, D. Li, Y.-G. Yin, Inorg. Chim. Acta 360 (2007) 588.

[31] M. Espino Lizarraga, R. Navarro, E.P. Urrolabeitia, J. Organomet. Chem. 542 (1997) 51.

[32] A. Sousa-Pedrares, M. Luz Durán, J. Romero, J.A. García-Vázquez, J.C. Monteagudo, A. Sousa, J.R. Dilworth, Inorg. Chim. Acta 359 (2006) 863.

[33] A.R. Cowley, R.J. Dilworth, C.A. Maresca von Beckh, Acta Crystallogr. E61 (2005) m1237.

[34] A. Bondi, J. Phys. Chem. 68 (1964) 441.

[35] N.L. Allinger, J.A. Hirsch, M.A. Miller, I.J. Tyminski, F.A. Van-Catledge, J. Am. Chem. Soc. 90 (1968) 1199.